Drug Design, Development and Therapy

Dovepress
open access to scientific and medical research

Open Access Full Text Article

ORIGINAL RESEARCH

Prunella vulgaris L. Attenuates Experimental Autoimmune Thyroiditis by Inhibiting HMGB1/TLR9 Signaling

Qingling Guo[1,2]
Haili Qu[3]
Hong Zhang[4]
Xia Zhong[4]

[1]Department of Endocrinology, Shandong Provincial Hospital Affiliated to Shandong First Medical University, Jinan, 250021, People's Republic of China; [2]Department of Endocrinology, Shandong Provincial Hospital, Cheeloo College of Medicine, Shandong University, Jinan, 250012, People's Republic of China; [3]Department of Nursing, Shandong Provincial Hospital Affiliated to Shandong First Medical University, Jinan, 250021, People's Republic of China; [4]Department of General Practice, Shandong Provincial Hospital Affiliated to Shandong First Medical University, Jinan, 250021, People's Republic of China

Background: *Prunella vulgaris* L. (PV) has been used to treat autoimmune thyroiditis (AIT), but the underlying mechanism remains unknown. The present study was designed to evaluate the effect of PV on AIT and explore the role of high-mobility group box-1 (HMGB1) signaling in PV-mediated effects in vivo and in vitro.

Methods: In the present study, bioactive components of PV were identified using UPLC-ESI-MS. The protective effects and potential mechanisms critical for the anti-inflammatory and immunomodulatory effects of PV in AIT were investigated in a rat model of thyroglobulin-induced experimental autoimmune thyroiditis (EAT) and in lipopolysaccharide (LPS)-induced thyroid follicular cells (TFCs).

Results: The main bioactive compound identified in PV was rosmarinic acid. The thyroid volume, thyroiditis inflammation score and serum thyroglobulin antibody levels of EAT rats were attenuated by PV treatment ($P<0.01$). In addition, PV significantly reduced the elevated levels of the proinflammatory cytokines TNF-α, IL-6, IL-1β and monocyte chemoattractant protein-1 (MCP-1) both in vivo ($P<0.01$) and in vitro ($P<0.05$). PV downregulated HMGB1 mRNA and protein expression, reduced HMGB1 secretion, and inhibited TLR9 signaling pathways (TLR9 and MyD88) in PV-treated EAT rats and TFCs. Moreover, PV reversed the increases in the numbers of splenic Th1, Th2, and Th17 cells. Finally, our results acquired following administration of ethyl pyruvate, an HMGB1 inhibitor, to splenocytes cultured in vitro supported the hypothesis that the HMGB1/TLR9 pathway is involved in the PV-mediated reductions in Th1, Th2 and Th17 cells.

Conclusion: PV decreased the activity of the TLR9/MyD88 pathway and proinflammatory cytokines through HMGB1. In addition, we are the first to show that PV attenuated the HMGB1-induced increases in Th1, Th2 and Th17 cells in AIT models. These findings provide new evidence for the potential therapeutic value of PV as a treatment for AIT and other autoimmune diseases.

Keywords: autoimmune thyroiditis, *Prunella vulgaris* L., HMGB1, TLR9

Introduction

Autoimmune thyroiditis (AIT) is an organ-specific autoimmune disease characterized by the infiltration of lymphocytes into the thyroid gland. It is now recognized as the most frequent autoimmune thyroid disorder and the most common cause of acquired hypothyroidism.[1] Genetic susceptibility and environmental risk factors contribute to the loss of immune tolerance and dysregulation of the immune system.[2] Excessively stimulated $CD4^+$ T cells are known to play the main role in the pathogenesis of AIT.[3] However, the fundamental mechanism of AIT remains

Correspondence: Xia Zhong
Department of General Practice, Shandong Provincial Hospital Affiliated to Shandong First Medical University, No. 324 Jingwu Road, Huaiyin Distinct, Jinan, Shandong Province, 250021, People's Republic of China
Email zxbs1231@126.com

Received: 21 June 2021
Accepted: 28 September 2021
Published: 4 November 2021

Graphical Abstract

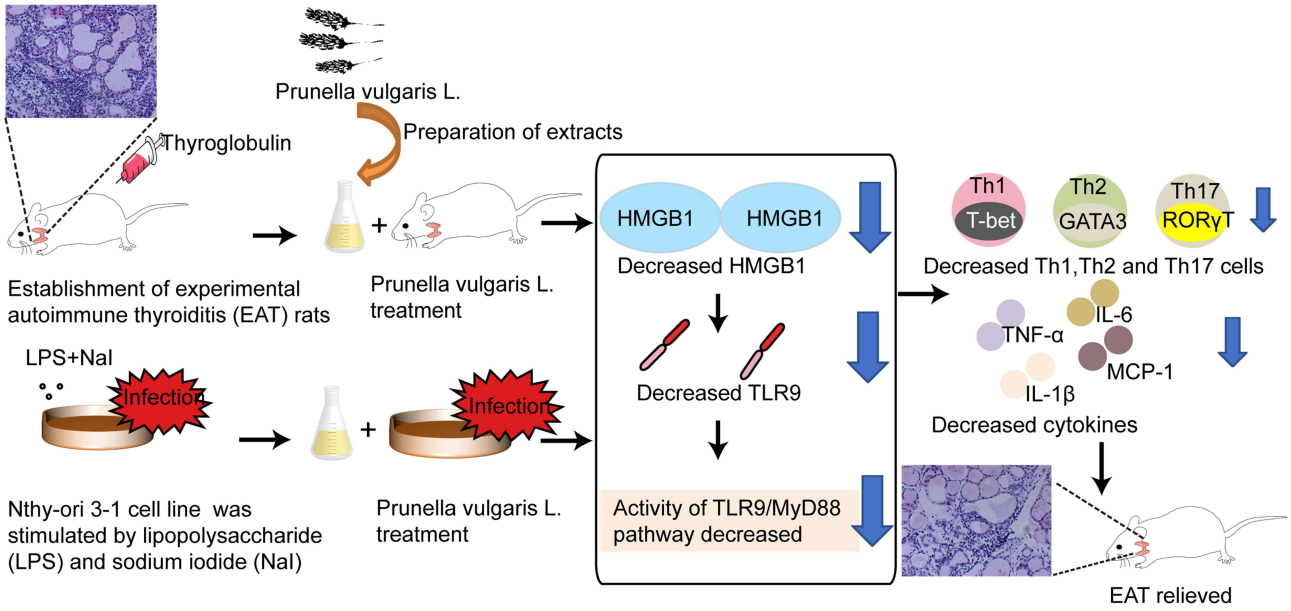

unclear. Synthetic LT-4, which is the first-line treatment for hypothyroidism caused by thyroiditis, is not curative.[4] Therefore, studies aiming to elucidate the pathogenesis of AIT and identify new therapies for AIT are urgently needed.

Extracellular high-mobility group box-1 (HMGB1) is usually categorized as a nonhistone protein that is mainly located in the nucleus and modulates chromosomal architecture.[5] In the contexts of cell stress or damage, HMGB1 can be transferred extracellularly and function as a damage-associated molecular pattern (DAMP), playing vital roles in the initiation and progression of inflammation and autoimmunity.[6] HMGB1 can interact with multiple pattern recognition receptors, among which Toll-like receptor (TLR) 9, has been widely studied and recognized as effective HMGB1 receptors.[7] Once stimulated by ligands, TLR9 recruits downstream adaptor molecules, including myeloid differentiation factor 88 (MyD88), resulting in the production of multiple proinflammatory cytokines, such as interleukin (IL)-6 and tumor necrosis factor-α (TNF-α).[8] Previous studies have shown that the HMGB1/TLR/MyD88 pathway may play important roles in the pathogenesis of AIT.[6,9] Accordingly, searching for drugs that modulate HMGB1/TLR9-mediated inflammation may yield promising strategies for curing AIT.

Prunella vulgaris L. (PV), commonly known as "Xiakucao" in China, is a perennial herbaceous plant that belongs to the Labiatae family. It has been widely used to treat upper respiratory infections, colds, sore throat, headache, and swelling of the thyroid gland with remarkable clinical efficacy.[10] Its pharmacological anti-inflammatory and immunoregulatory effects are receiving increasing attention from researchers. Furthermore, PV and its preparations have been reported to reduce serum autoantibody titers and thyroid volume in AIT patients in several clinical studies from China.[11,12] In addition, a previous study by our team confirmed that PV efficiently decreased the inflammation score for the thyroid, anti-thyroglobulin antibody (TgAb) levels and thyroid volume in experimental autoimmune thyroiditis (EAT) rats through indoleamine 2,3-dioxygenase 1-induced expansion of regulatory T cells.[13] However, whether PV influences the HMGB1/TLR9 pathway remains unclear.

Therefore, the purpose of this study was to observe the effects of PV on AIT and explore the mechanism underlying the effects. To investigate the hypothesis that PV ameliorates AIT by regulating the activity of HMGB1/TLR9 pathway components and correspondingly influencing proinflammatory cytokines and T helper (Th) cell

subsets, we established an EAT model in Tg-immunized Lewis rats and evaluated cultured Nthy-ori 3–1 thyroid follicular cells (TFCs) in vitro. Our findings may reveal the potential therapeutic value of PV in AIT and promote the possible research and clinical applications of PV.

Materials and Methods

Plants and Preparation of Extracts

PV used in this study was collected from Nayong County, Bijie City, Guizhou Province, China (105.39 E, 26.78 N) in July 2018 and identified by two professional pharmacists (Specimen No. 2017112; deposited in the Laboratory of Traditional Chinese Medicine, Guiyang Xintian Pharmaceutical Co., Ltd., Guizhou, China). As described previously,[13] PV aqueous extracts were prepared at Guiyang Xintian Pharmaceutical Co., Ltd. In brief, fresh fruiting spikes were cleaned, air-dried and ground into powder on a 40-mesh screen. Two hundred grams of raw material was soaked in a moderate amount of distilled water at 70 °C, and the sample was processed by condensation for two hours. The condensation process was repeated three times. Then, the extracts were combined and filtered three times through Whatman No. 1 filter paper. The filtrate was concentrated and lyophilized. The cold-dry powder was dissolved in 1 L of saline and stored hermetically at 4°C. The aqueous extracts were sterilized by filtration and disinfected using a gel-clot Limulus amebocyte lysate assay before use. The recommended daily consumption of crude PV is 0.2−0.4 g per kg body weight, which was approximately equal to 1−2 mL of the prepared aqueous extract.

Ultra-Pressure Liquid Chromatography-Electrospray Ionization-Mass Spectrometry (UPLC-ESI-MS)

We performed UPLC-ESI-MS to identify the chemical composition of the aqueous extracts of PV using an LCMS-8050 series mass spectrometer. The analytical instrument was equipped with a Waters ACQUITY HSS T3 column (100*2.1 mm I.D.; 1.8 μM particle size; Waters, USA). The UPLC system was coupled to a 5500 triple quadrupole mass spectrometer equipped with an ESI source (Sciex, Framingham, MA). Chemical separation was performed using a mobile phase consisting of 0.5% formic acid in double-distilled water (solvent A) and acetonitrile (solvent B at 25 °C). Gradient elution conditions were performed at a flow rate of 0.4 mL/min, with 0−5 min of 5–10% solvent A, 5−8 min of 10–35% solvent A, and 8−20 min of 35–65% solvent A. ESI-MS was performed in the negative ion detection mode. The injection volume was 2 μL using the full loop injection mode. Nitrogen was used for atomization and as a dry gas at flow rates of 3.0 L/min and 1 L/min, respectively. The collision gas was argon at a collision voltage of 35 V. The interface temperature was 300 °C, and the DL temperature was 250 °C. The hot gas flow rate was 10 L/min in a 400 °C temperature block.

Rats and Groups

Six-week-old female Lewis rats (LEW/Crl-113) were purchased from Weitonglihua Biotech and raised in a specific pathogen-free environment in the Experimental Animal Center at the Shandong Provincial Hospital Affiliated to Shandong First Medical University. All experimental procedures were approved by the Experimental Animal Management Committee of Shandong Provincial Hospital.

Experiment One: Construction of an experimental autoimmune thyroiditis (EAT) Rat Model and PV Treatment

After acclimation for 1 week, rats (n = 36) were randomly divided into 2 groups: the normal group (NC, sterile distilled water, n = 12) and the EAT MODEL group (EAT MODEL, distilled water containing 0.05% sodium iodide (NaI), n=24) (NaI, Tianjin Damao Chemical Reagent Factory). After this initial treatment, the 24 rats were immunized with 200 μL of pig thyroglobulin (pTg)/complete Freund's adjuvant (CFA) mixture (0.2 mg/mL) in the 2nd and 6th weeks (pTg, Sigma, lot number: SLBW7430; CFA: Sigma, lot number: 018K7012). At the end of the 8th week, TgAbs were detected to confirm successful establishment of the EAT model. Then, the EAT MODEL group was divided into two groups: the PV treatment group (EAT +PV, n=12) and the model group (EAT, n=12), which were administered PV at a dosage of 2 mL/kg or an equivalent volume of phosphate-buffered saline (PBS), respectively, once a day for another 12 weeks until sacrifice. In addition, the rats in the NC group were orally administered distilled water until sacrifice. Thyroid tissues were removed, washed with cold saline, dried on a pad of filter paper and weighed on an electronic balance. Fresh spleen tissues from rats in the 3 groups were homogenized into single-cell suspensions for flow cytometric analysis. The animal experimental design is shown in Figure 1A.

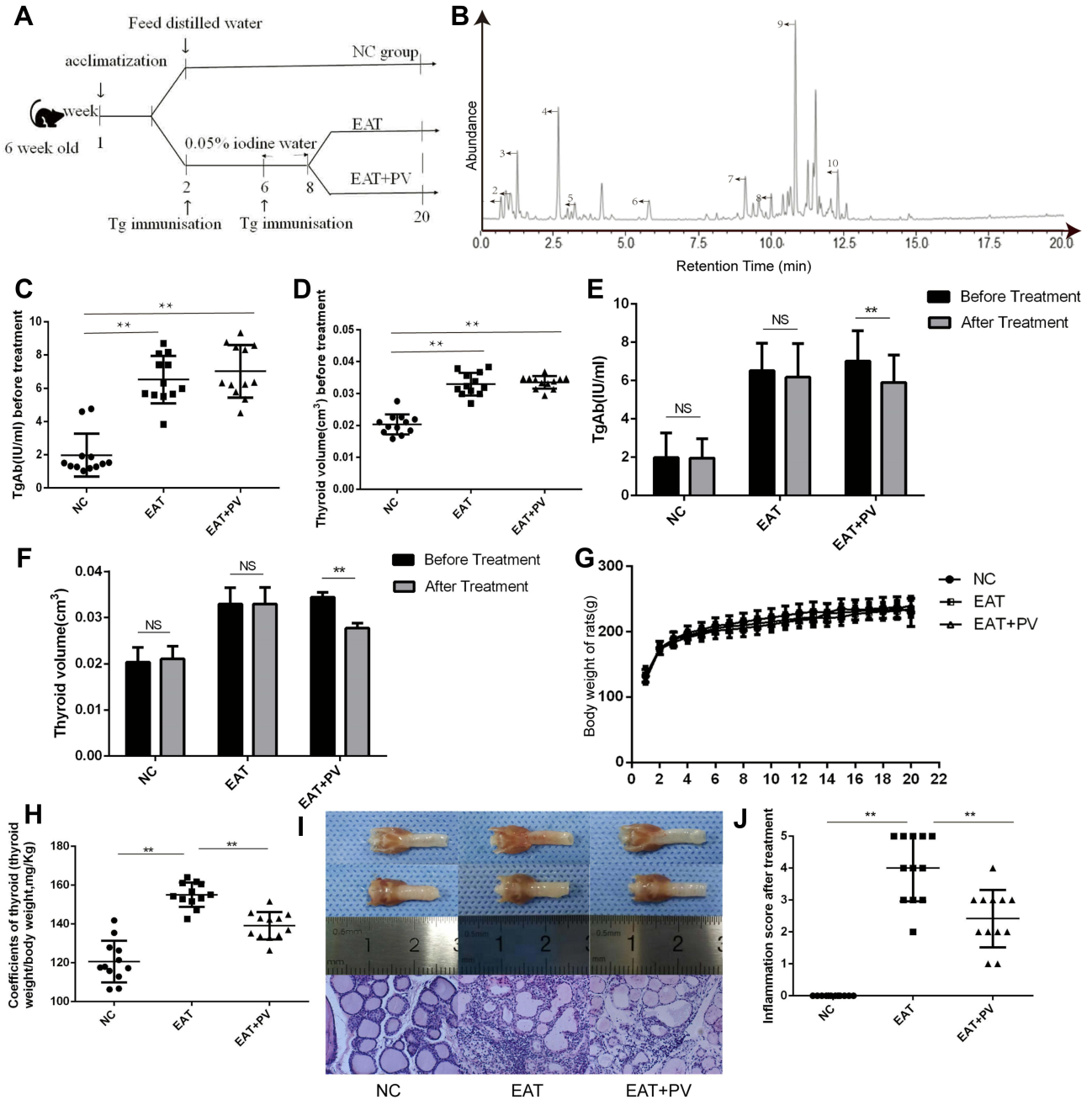

Figure 1 UPLC-ESI-MS chromatogram of PV extracts and the therapeutic effect of PV on EAT rats. (**A**) Schematic of the experimental processes. (**B**) UPLC-ESI-MS chromatogram of PV extracts. (**C**) Serum TgAb levels measured by ELISA before PV treatment (at the 8th week). (**D**) Thyroid volume calculated by ultrasonic index before PV treatment (at the 8th week). (**E**) Serum TgAb levels and thyroid volume. (**F**) before and after PV treatment (at the 20th week). (**G**) Body weight and (**H**) coefficients of thyroid (thyroid weight/body weight) of rats among groups. (**I**) Representative morphologic images of thyroid tissues from randomly selected rats in the three groups (HE staining and 200×magnification). (**J**) Inflammation scores of thyroid among groups (at the 20th week). The data are presented as the mean ± SD (n=12 per group). Differences among the groups were analysed using ANOVA. Comparisons before and after treatment were analyzed using paired t-tests. Chi-squared test was performed to compare the inflammatory scores. **, P<0.01.

Abbreviations: NS, no significant difference; NC, normal control group; EAT, experimental autoimmune thyroiditis rats administered PBS; EAT+PV, EAT rats administered PV extracts.

Experiment Two: In vitro Splenocyte Culture and Treatment

After acclimation for 1 week, 48 female Lewis rats were randomly separated into 2 different groups: the normal group (NC, sterile distilled water, n = 8) and the in vitro-EAT MODEL group (EAT MODEL, distilled water containing 0.05% NaI, n =40). The EAT rat model was constructed as described above. At the end of the 8th week, all rats were sacrificed. Fresh spleen tissues were collected from rats in the 2 groups and passed through 200-gauge stainless steel mesh

above a dish filled with PBS. All isolated splenocytes were harvested and homogenized into single-cell suspensions. Spleen mononuclear cells were isolated using Ficoll-Hypaque density centrifugation (TBD, lot number: LTS1083-200). Next, spleen mononuclear cells were resuspended in RPMI 1640 medium supplemented with 10% fetal bovine serum, seeded in 6-well (2×10^6/well) culture plates, and incubated in a humidified atmosphere at 37 °C containing 5% CO_2.

Splenocytes cultured in vitro were divided into the following 6 groups:

A, the in vitro-NC group, which received medium only;

B, the in vitro-NC+PV group, which received 5 μmol/L PV;

C, the in vitro-EAT group, which received medium only;

D, the in vitro-EAT+PV group, which received 5 μmol/L PV;

E, the in vitro-EAT+ ethyl pyruvate (EP), which received 5 mmol/L EP; and

F, the in vitro-EAT+PV+EP group, which received 5 μmol/L PV and 5 mmol/L EP.

TFC Culture and Drug Administration

The Nthy-ori 3–1 cell line was obtained from the China Center Type Culture Collection (Wuhan, China). Cells were cultured in RPMI 1640 medium supplemented with 2 mM glutamine and 10% fetal bovine serum in a humidified atmosphere containing 5% CO2. Cells between passage 5 and passage 12 were used for all experiments. The cells were divided into the following six groups:

A, the normal control (Con) group, which received medium only;

B, the Con +PV group, which received 5 μmol/L PV;

C, the lipopolysaccharide (LPS)+ NaI group, which received 10 μg/mL LPS (Sigma) and 100 mg/L NaI;

D, the LPS+NaI +PV group, which received 10 μg/mL LPS + 1×10^{-2} mmol/L NaI + 5 μmol/L PV;

E, the LPS + NaI+ EP group, which received 10 μg/mL LPS+1×10^{-2} mmol/L NaI + 5 mmol/L EP; and

F, the LPS+NaI+PV+EP group, which received 10 μg/mL LPS +1×10^{-2} mmol/L NaI + 5 μmol/L PV+ 5 mmol/L EP.

Thyroid Ultrasound Imaging

Twenty-four hours after the last administration of PV, the rats in experiment one were intraperitoneally injected with 2% sodium pentobarbital (70 mg/kg); next, the limbs and teeth of the rats were fixed on a board, and the fur at the neck was removed. Thyroids were analyzed using a GE logic E9 ultrasonography system by two designated experienced technicians. The transverse (a), longitudinal (b) and thick (c) diameters of the thyroid of each rat were obtained using ultrasonography. Thyroid volume was calculated using the following formula: $\frac{\pi}{6}(a\times b\times c)$. Total thyroid volume included the two lobes and the isthmus.

Hematoxylin and Eosin (HE) Staining

All rats in experiment one were anesthetized and sacrificed at the end of the 20th week. The thyroid was removed and fixed in a 4% paraformaldehyde solution for 8 h. Then, the thyroid was routinely dehydrated, embedded in paraffin and cut into 4-μm-thick sections for routine HE staining. The degree of infiltration of the thyroid tissue by inflammatory cells was observed under a light microscope at 200× magnification. The scoring standards were described previously.[13]

Enzyme-Linked Immunosorbent Assay (ELISA)

Twenty-four hours after the last administration, 2 mL of venous blood was collected from each experimental rat by subclavian venipuncture. The concentrations of TgAbs, HMGB1, TNF-α, IL-6, IL-1β and monocyte chemoattractant protein-1 (MCP-1) in rats were detected with ELISA kits according to the manufacturer's protocol (TgAbs: #m1003044, Kangting, Tianjin, China; HMGB1: E-EL-R0505c, Elabscience, China; TNF-α: EK382/3-96, Multisciences, China; IL-6: ER306/3-96, China; IL-1β: E-EL-R0012c, Elabscience, China; MCP-1: E-EL-R0633c, Elabscience, China). The secretion of HMGB1, TNF-α, IL-6, IL-1β and MCP-1 by cell lines was detected with ELISA kits according to the manufacturer's protocol (HMGB1: E-EL-H1554c, Elabscience, China; TNF-α, EK182HS-48, Multisciences, China; IL-6, EK106/2-48, Multisciences, China; IL-1β: E-EL-H0149c, Elabscience, China; MCP-1: E-EL-H6005, Elabscience, China).

Real-Time Polymerase Chain Reaction (RT-PCR)

Total RNA was extracted from thyroid tissues and cell lines using TRIzol reagent (#9109; TaKaRa, Japan) according to the manufacturer's instructions. RNA concentrations were measured using a NanoDrop 1000 spectrophotometer (NanoDrop, USA). Total RNA was reverse

transcribed into cDNA templates with the PrimeScript™ RT Reagent Kit with gDNA Eraser (TaKaRa, Kusatsu, Japan) according to the instruction manual. Using the cDNAs templates, the mRNA levels of the HMGB1, TLR9, MyD88, t-box expressed in T cells (T-bet), GATA binding protein 3 (GATA3) and retinoic acid receptor-related orphan nuclear receptor γt (RORγT) genes in rat thyroids and TFCs were assessed using real-time quantitative PCR (qPCR) in a 20-μL reaction system containing 10 μL of SYBR green mix (Bestar qPCR Master Mix, DBI, Germany), 1 μL of cDNAs, 1 μL of each primer (10 mmol/L), and 7 μL of RNase-free ddH_2O. qPCR was performed using a Roche 480 fluorescent polymerase chain analyzer with the following program: 95 °C for 30 s, followed by 40 cycles at 95 °C for 5 s and 60 °C for 30 s. β-Actin was chosen as a housekeeping gene for internal reference. Table 1 shows the primer sequences and amplicon lengths.

Table 1 Primer Sequences for Quantitative Real-Time PCR

Gene Name	Organism	Sequences (5′- 3′)
HMGB1	Rat	F: TCTGTTCTGAGTACCGCCCA R: TCGCAACATCACCAATGGA
TLR9	Rat	F: GAGTGCTTGATGTGGGTGGG R: TTAGGTCCAGCACCGAGAGG
MyD88	Rat	F: GCTGAGAGGAAGAGTTCTAC R: CAGTGATAACCCTGGACTAC
T-bet	Rat	F: GGGTTGGAGGTGTCGGGGAAGC R: CCCGGCCACAGTGAAGGACAGG
GATA-3	Rat	F:CCGCCTCGCCCTGGAACCTC R: CCCGCAGCCAGAGAAGAGGATGA
RORγt	Rat	F: ATGCTAGCCCCGATGTCTTCAAAT R: TGTCGTCCGCATAGGGCTCTTA
β-actin	Rat	F: GGAGATTACTGCCCTGGCTCCTA R: GACTCATCGTACTCCTGCTTGCTG
HMGB1	Homo sapiens	F: TGCAGATGACAAGCAGCCTT R: GCTGCATCAGGCTTTCCTTT
TLR9	Homo sapiens	F: CCCTGCCCTACGTATGCCT R: ACGTCCTTGCGGTCCTCC
MyD88	Homo sapiens	F: GCATGGAACCAGTGGCTGTGAG R: GAGGAAGTGGAATGGGCGGTGT
β-actin	Homo sapiens	F: CCTGGCACCCAGCACAAT R: GCTGATCCACATCTGCTGGAA

Abbreviations: F, forward; R, reverse.

Western Blot Analysis

The protein levels of HMGB1 (Proteintech, catalog number: 10829-1-AP), TLR9 (Abcam, catalog number: ab52967), and MyD88 (Santa, catalog number:Sc-74532) in rat thyroids and TFCs were detected by Western blotting. The thyroid was immediately collected in liquid nitrogen and stored at −80 °C. Next, the thyroid was lysed in RIPA lysis buffer containing protease inhibitors and phosphatase inhibitors to extract total proteins. The protein concentration was measured using the BCA Protein Quantitative Assay Kit. Proteins were separated at a constant voltage of 110 V and then transferred to PVDF membranes. After blocking with 5% skim milk, the membranes were incubated overnight at 4 °C with a primary antibody diluted in the blocking solution, followed by incubation with a horseradish peroxidase-conjugated secondary antibody for another 1 h. Densitometry values indicative of relative target protein expression levels were normalized to the values for β-actin on the same membrane. Immunoreactive proteins were reacted with an enhanced chemiluminescence solution after washing and visualized using SuperSignal West Pico Chemiluminescent Substrate (Thermo Scientific, Rockford, IL, USA).

Flow Cytometry

The density of spleen mononuclear cells was adjusted to 1×10^6 cells/mL in each tube. Cells were stimulated with Cell Activation Cocktail (with Brefeldin A) (Cell Activation Cocktail: 423303, BioLegend) and incubated at 37 °C in the presence of 5% CO_2 for 5 h. Then, for surface staining, the cells were stained with an anti-rat CD4-PE/Cy7 antibody (BioLegend, catalog number: 201516) for 30 min at 4 °C in the dark and then fixed and permeabilized for intracellular staining. Fixation was performed with fixation buffer (eBioscience, catalog number: 00–8222-49), and permeabilization was performed with permeabilization buffer (eBioscience, catalog number: 00–8333). For intracellular staining, anti-rat IFNγ-Alexa Fluor 647 (BioLegend, catalog number: 507810), anti-rat IL-4-PE (BioLegend, catalog number: 511905) and anti-rat IL-17A-FITC (11–7177-81, eBioscience) antibodies were added to the bottom of the tube and incubated for 30 min at 4 °C in the dark. After staining, the cells were washed with PBS twice. Data were acquired using an LSR Fortessa four-laser flow cytometer (BD Biosciences) and analyzed using FlowJo software (TreeStar Inc., Ashland, OR, USA).

Table 2 Compounds Identified in PV Extracts Using UPLC-ESI-MS

No.	Retention Time	Compound Name	M/C	Molecular Formula
1	0.88	Gluconic acid	195, 177, 159	$C_6H_{12}O_7$
2	1.05	Malic acid	133	$C_4H_6O_5$
3	1.26	Citric acid	191, 137	$C_6H_8O_7$
4	2.65	Long-chain fatty acid	395, 297, 320	$C_3H_6O_2$
5	3.25	Protocatechuic acid	153	$C_7H_6O_4$
6	5.85	Protocatechuic aldehyde	137	$C_7H_6O_3$
7	9.17	Caffeic acid	179	$C_9H_8O_4$
8	10.05	Isorosmarinic acid glycoside	521, 117, 135, 179	$C_{24}H_{26}O_{13}$
9	10.88	Rosmarinic acid	359, 322	$C_{18}H_{16}O_8$
10	12.10	Ursolic acid	491, 135, 183	$C_{30}H_{48}O_3$

Abbreviations: UPLC-ESI-MS, ultra-pressure liquid chromatography-electrospray ionization mass spectrometry; PV, Prunella vulgaris; M/C, mass-to-charge ratio.

Statistical Analysis

Statistical analyses were performed with SPSS 21.0 software. Quantitative variables are presented as the means ± standard deviations (SD). Student's *t*-test was used to analyze differences between two groups. Comparisons among groups were conducted using one-way ANOVA. $P<0.05$ was considered statistically significant.

Results

Identification of Bioactive Components of PV

As shown in Figure 1B, the UPLC-ESI-MS chromatographic peaks were well separated. Ten chromatographic peaks were identified in the multilevel mass spectrometry profile according to mass weight (Table 2). The data suggested that rosmarinic acid was the main component of aqueous *P. vulgaris* extracts.

PV Ameliorated EAT

Changes in serum TgAb levels and thyroid volume were evaluated at the end of the 8th week before treatment to confirm the successful establishment of the rat EAT model. Compared with the NC group, the EAT and EAT+PV groups showed a more than 3-fold increase in serum TgAb levels and a 1.75-fold increase in thyroid volume (Figure 1C and D). No differences were found in the TgAb level or thyroid volume between the EAT and EAT+PV groups.

After PV treatment for 12 weeks, serum TgAb levels and thyroid volume decreased significantly compared with the values before treatment (P <0.01, Figure 1E and F). PV treatment reduced serum TgAb levels by 16% and thyroid volume by 19.5%. At the end of the 20th week, the rats were sacrificed, and the thyroid weight-to-body weight percentage was calculated. The weight percentages were significantly decreased without loss of body weight after PV treatment (Figure 1G and H). This result was consistent with the changes in thyroid volume observed using ultrasonography.

According to HE staining images (Figure 1I), little infiltration of lymphocytes and plasma cells between the follicles in the thyroid was observed in the NC group. In comparison, in the EAT group, many thyroid follicles were destroyed, atrophied and infiltrated with a large number of lymphocytes. Furthermore, the infiltration of lymphocytes between the follicles was alleviated after PV treatment in EAT rats. In addition, PV administration significantly decreased thyroid inflammation scores in EAT rats (Figure 1J). Based on the results above, the aqueous PV extract attenuated both thyroiditis and goiter in the rat EAT model.

PV Downregulated HMGB1 Expression

To explore the influence of PV on HMGB1 expression, serum HMGB1 levels were determined by ELISA. As shown in Figure 2A, PV administration significantly reduced serum HMGB1 levels in EAT rats ($P<0.05$). Furthermore, the mRNA and protein expression of HMGB1 in the thyroid glands was also detected. Elevated HMGB1 mRNA ($P<0.01$, Figure 2B) and protein ($P<0.01$, Figure 2C) expression in the thyroid was observed in EAT rats compared with NC rats. However, HMGB1 expression was remarkably decreased ($P<0.01$ for both mRNA and protein) in the EAT+PV group after PV administration.

We also assayed HMGB1 expression in TFCs and cell supernatants. As shown in Figure 2D, the levels of HMGB1 in the LPS combined with NaI-treated cells were significantly higher than those in control cells ($P<0.01$), and the HMGB1 inhibitors EP and PV both partially suppressed LPS-induced HMGB1 overexpression. Moreover, treating the cells with

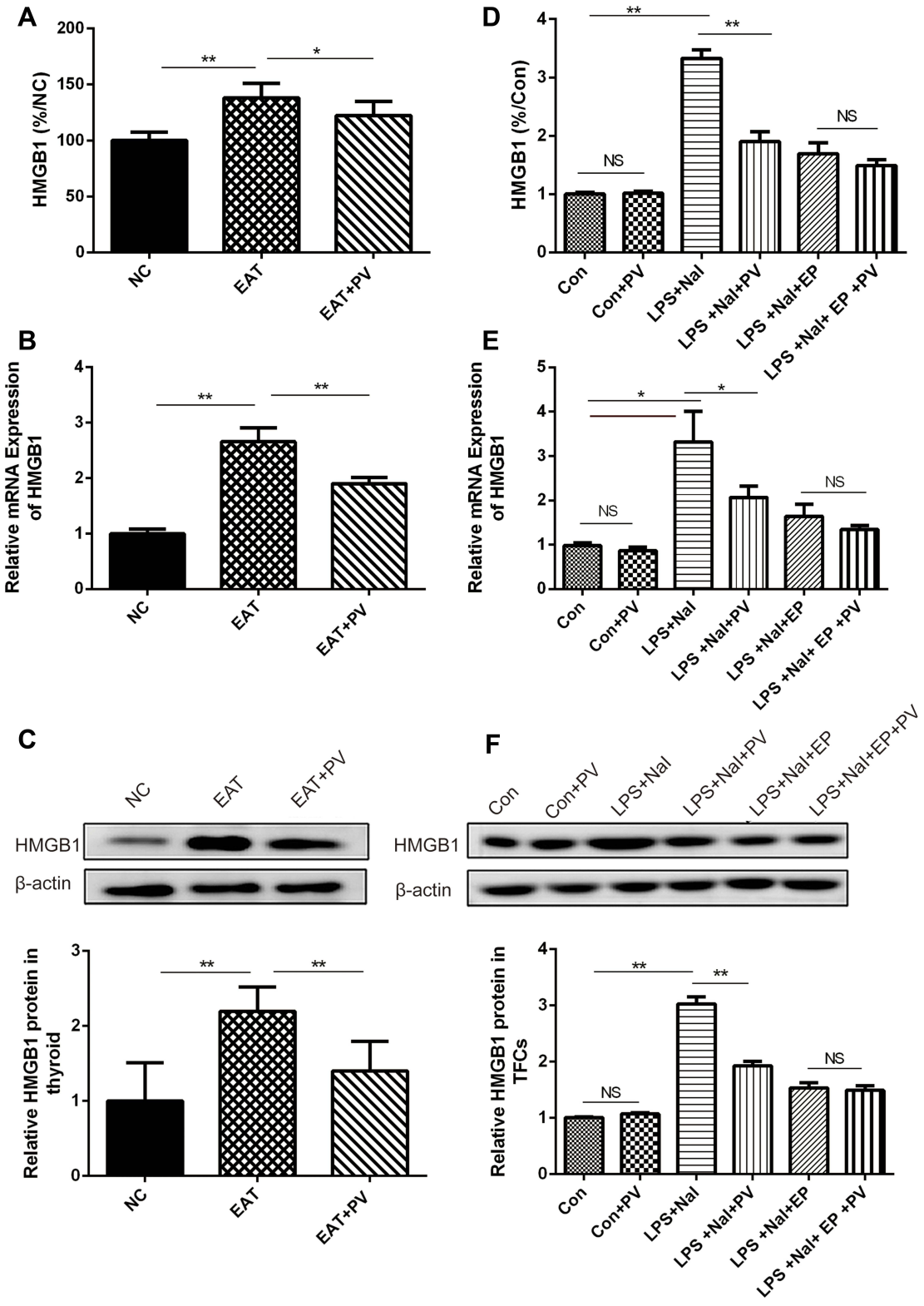

Figure 2 PV downregulated HMGB1 expression. (**A**) HMGB1 levels in serum from rats were detected using ELISA (n=8 per group). Relative expression levels of HMGB1 mRNA (**B**) and protein (**C**) in the thyroid from rats were determined using PCR and Western blotting, respectively. (**D**)The levels of HMGB1 in the supernatant of Nthy-roi 3–1 cells were detected by ELISA (data from three independent experiments). The relative levels of HMGB1 mRNA (**E**) and protein (**F**) in Nthy-roi 3–1 cells were determined using PCR and Western blotting, respectively. The data are presented as the mean ± SD. Pairwise statistical comparisons among groups were performed using ANOVA and Bonferroni corrections. *P<0.05; **, P<0.01.

Abbreviations: NS, no significant difference; NC, normal control group; EAT, experimental autoimmune thyroiditis rats administered PBS; EAT+PV, EAT rats administered PV extracts; Con, control cells; Con+PV, control cells treated with PV; LPS+Nal, cells stimulated with lipopolysaccharide and sodium iodide; LPS+Nal+PV, stimulated cells treated with PV; LPS+Nal+EP, stimulated cells treated with ethyl pyruvate; LPS+Nal+EP+PV, stimulated cells treated with ethyl pyruvate combined PV.

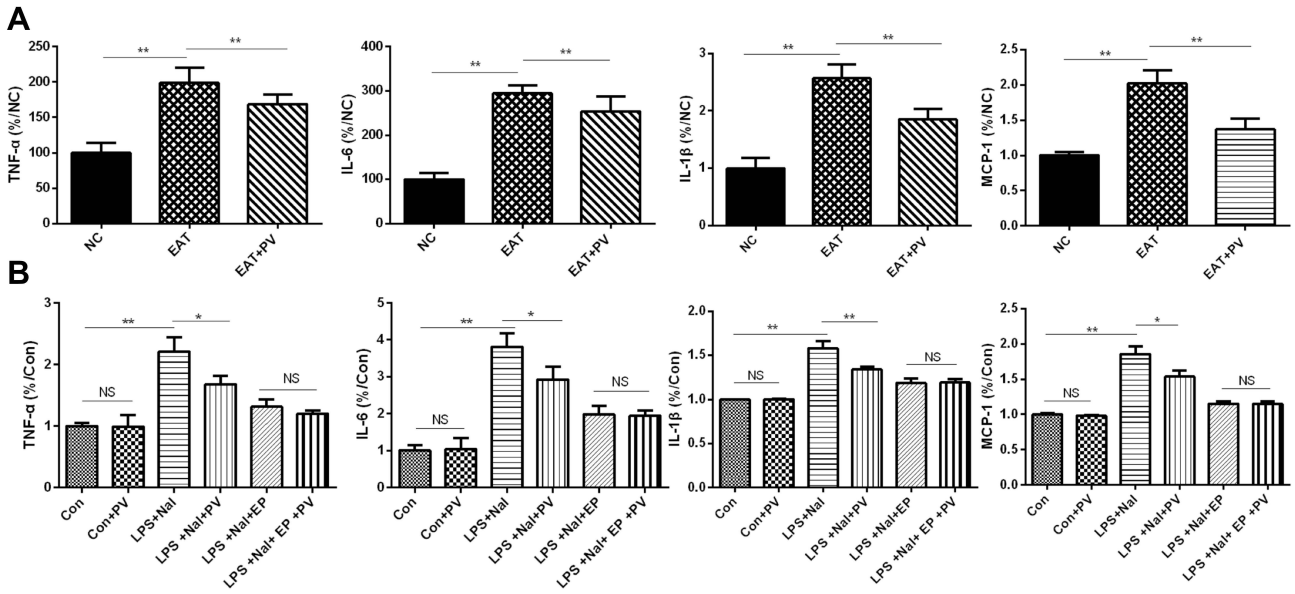

Figure 3 PV reduced proinflammatory cytokine levels. (**A**) The TNF-α, IL-6, IL-1β and MCP-1 levels in serum from rats (n=8 in each group) and (**B**) in the supernatant of Nthy-roi 3–1 cells (data from three independent experiments) were determined using ELISAs. The data are presented as the mean ± SD. Differences among the groups were compared using ANOVA. *P<0.05; **, P<0.01.

Abbreviations: NS, no significant difference; NC, normal control group; EAT, experimental autoimmune thyroiditis rats administered PBS; EAT+PV, EAT rats administered PV extracts. Con, control cells; Con+PV, control cells treated with PV; LPS+NaI, cells stimulated with lipopolysaccharide and sodium iodide; LPS+NaI+PV, stimulated cells treated with PV; LPS+NaI+EP, stimulated cells treated with ethyl pyruvate; LPS+NaI+EP+PV, stimulated cells treated with ethyl pyruvate combined PV.

a combination of EP and PV synergistically reversed the LPS-induced increases in HMGB1 expression. Consistent results were obtained for the mRNA and protein expression levels of HMGB1 (Figure 2E and F). In brief, PV downregulated HMGB1 mRNA and protein expression to an extent that was equal to that achieved with EP, which is recognized as an HMGB1 inhibitor.

PV Suppressed the Secretion of Proinflammatory Cytokines Through HMGB1

In vivo experiments revealed significant increases in the serum levels of TNF-α, IL-6, IL-1β and MCP-1 in the EAT group compared to the control group (P<0.01 for all cytokines, Figure 3A). However, the elevated cytokine levels were remarkably reversed after PV administration in the EAT+PV group (P<0.01 for all cytokines).

The in vitro experimental results suggested that the administration of LPS combined with NaI significantly increased the levels of TNF-α, IL-6, IL-1β and MCP-1 compared to control treatment (P<0.01 for all cytokines, Figure 3B). PV treatment significantly downregulated the cytokine elevations induced by LPS and NaI (P<0.01 for IL-1β and P<0.05 for TNF-α, IL-6 and MCP-1), although PV alone did not influence the cytokine levels in control TFCs (P>0.05).

We inhibited HMGB1 with EP and determined the cytokine levels in vitro to investigate whether PV inhibits cytokine secretion by regulating HMGB1. However, PV did not change the expression levels of TNF-α, IL-6, IL-1β or MCP-1 in the cells pretreated with EP (P > 0.05 for all).

PV Downregulated the TLR9/MyD88 Pathway Through HMGB1

We determined the effects of PV on the TLR9/MyD88 pathway to elucidate the mechanism underlying the thyroiditis alleviation mediated by PV in EAT rats. As shown in Figure 4A and B, the mRNA and protein expression levels of TLR9 and MyD88 in the EAT group were significantly higher than those in the NC group. PV administration effectively reduced the mRNA and protein expression of TLR9 and MyD88 in EAT rats (Figure 4A and B).

We determined the mRNA and protein levels of TLR9 and MyD88 in TFCs after inhibiting HMGB1 to investigate whether the PV-induced changes in the TLR9/MyD88 pathway were mediated by HMGB1. As shown in Figure 4C and D, PV alone did not change the expression levels of TLR9 or MyD88 in TFCs compared to control treatment (P>0.05 for both mRNA and protein), but PV

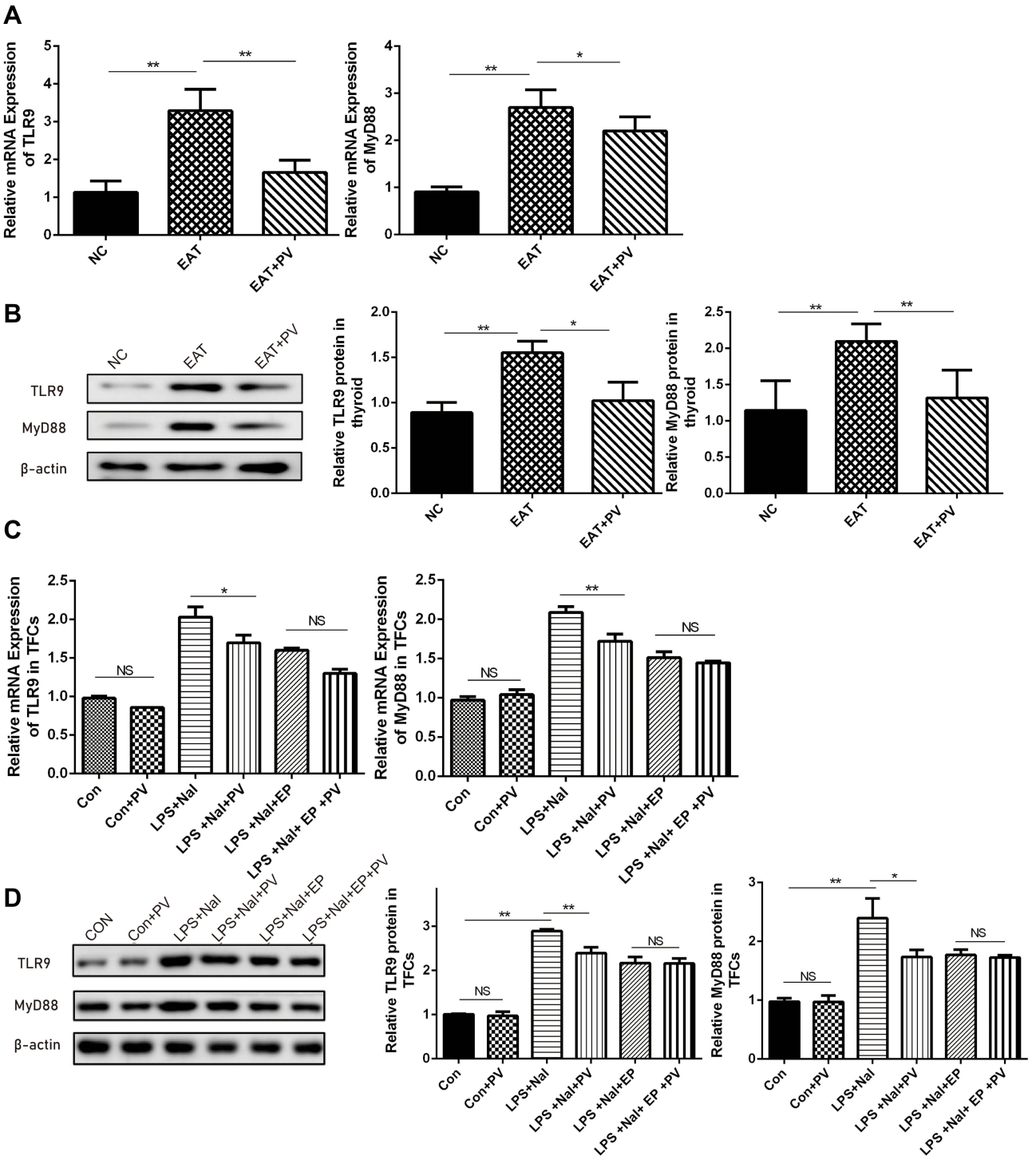

Figure 4 PV inhibited TLR9/MyD88 expression in vivo and in vitro. (**A**) Levels of TLR9 and MyD88 mRNA in thyroid tissues from rats were detected by PCR (n=8 in each group). (**B**) Representative images and quantitative analysis of TLR9 and MyD88 proteins in thyroid tissues from rats were detected by Western blot (n=8 in each group). (**C**) The TLR9 and MyD88 mRNAs in Nthy-roi 3–1 cells were detected by PCR (data from three independent experiments) (**D**) Western blot images and quantitative analysis of TLR9 and MyD88 proteins in Nthy-roi 3–1 cells. The data are presented as the mean ± SD. Pairwise statistical comparisons among groups were performed using ANOVA and Bonferroni corrections. *P<0.05; **, P<0.01.

Abbreviations: NS, no significant difference; NC, normal control group; EAT, experimental autoimmune thyroiditis rats administered PBS; EAT+PV, EAT rats administered PV extracts. Con, control cells; Con+PV, control cells treated with PV; LPS+NaI, cells stimulated with lipopolysaccharide and sodium iodide; LPS+NaI+PV, stimulated cells treated with PV; LPS+NaI+EP, stimulated cells treated with ethyl pyruvate; LPS+NaI+EP+PV, stimulated cells treated with ethyl pyruvate combined PV.

pretreatment significantly reduced TLR9 and MyD88 mRNA and protein expression in noninhibited cells compared to LPS+NaI-treated cells ($P<0.05$). On the other hand, cells treated with PV and EP did not display significant differences in the expression of TLR9 or MyD88 compared with cells treated with only EP ($P > 0.05$).

PV Reduced the Proportions of Th1, Th2, and Th17 Splenocytes by Inhibiting the HMGB1/TLR9 Pathway

We performed flow cytometry to measure the percentages of Th cell subsets. The percentages of Th1, Th2 and Th17 cell subsets among splenocytes from rats in the EAT group were remarkably higher than those in the NC group ($P <0.01$ for all subsets). However, the elevated percentages of Th1, Th2 and Th17 cell subsets were remarkably decreased in the EAT+PV group after PV treatment ($P<0.05$ for Th1, Figure 5A; $P<0.01$ for Th2, Figure 5B; and $P<0.01$ for Th17, Figure 5C). Furthermore, the mRNA levels of the specific transcription factors of Th1, Th2 and Th17 cells, T-bet, GATA3 and RORγT, respectively, were determined by RT-PCR (Figure 6). Our results indicated that the mRNA expression levels of T-bet, GATA3 and RORγT were significantly increased in the EAT group

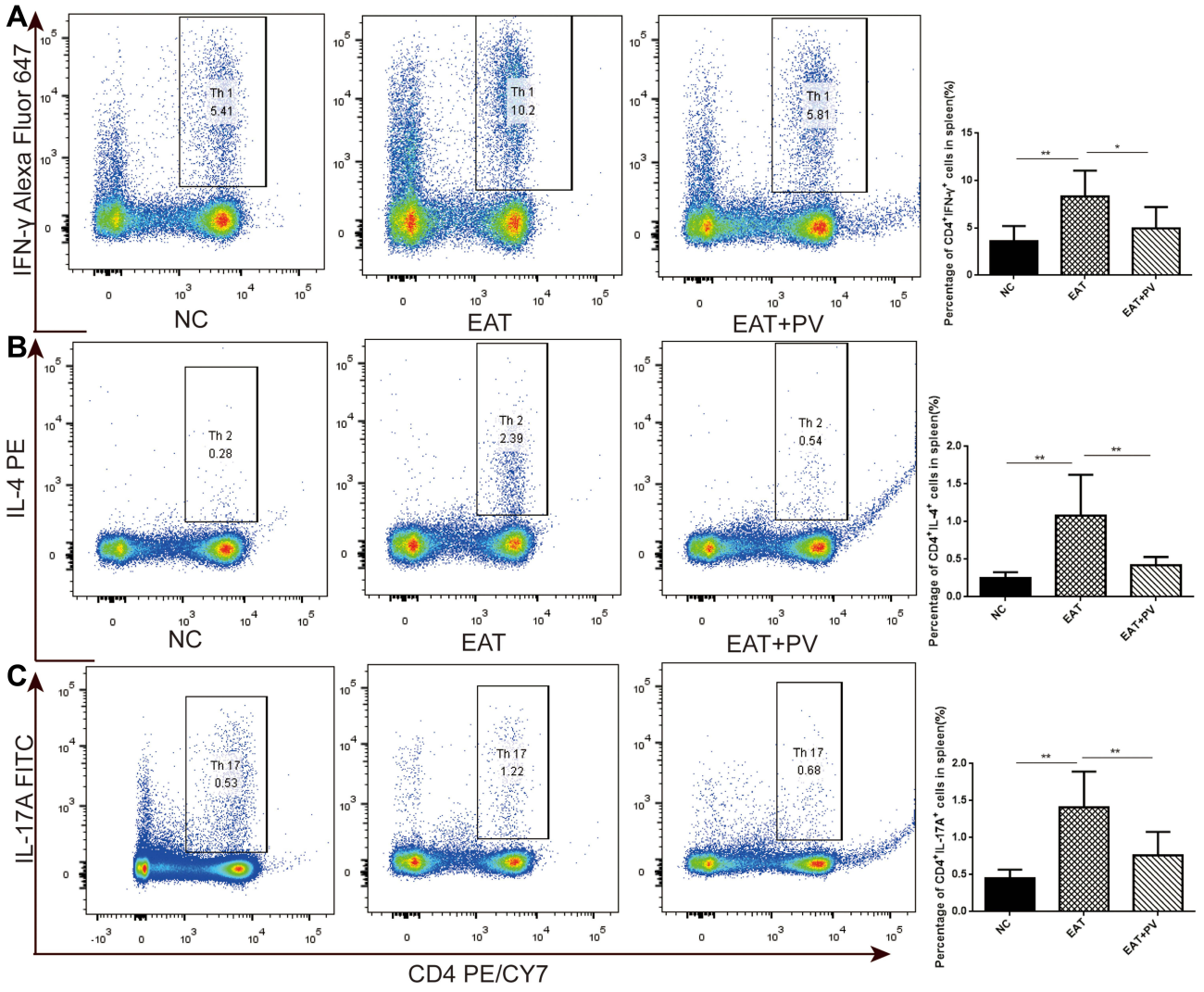

Figure 5 PV reduced the proportions of Th1/Th2/Th17 cells in splenocytes from EAT rats. (**A**) Subsets of Th1 cells in the $CD4^+$ gate were analyzed by performing intracellular staining for IFN-γ in splenocytes (left panels). The numbers in the right quadrants represent the percentage of $CD4^+IFN\text{-}\gamma^+$ cells in each group. (**B**) Subsets of Th2 cells in the $CD4^+$ gate were analyzed by performing intracellular staining for IL-4 in splenocytes (left panels). The numbers in the right quadrants represent the percentage of $CD4^+IL\text{-}4^+$ cells in each group. (**C**) Subsets of Th17 cells in the $CD4^+$ gate were analyzed by performing intracellular staining for IL-17A in splenocyte (left panels). The numbers in the right quadrants represent the percentage of $CD4^+IL\text{-}17^+$ cells in each group. The data are presented as the means ±SD (n=8 per group). Statistical comparisons among groups were performed using ANOVA. *$P<0.05$; **$P<0.01$.

Abbreviations: NC, normal control group; EAT, experimental autoimmune thyroiditis rats administered PBS; EAT+PV, EAT rats administered PV extracts.

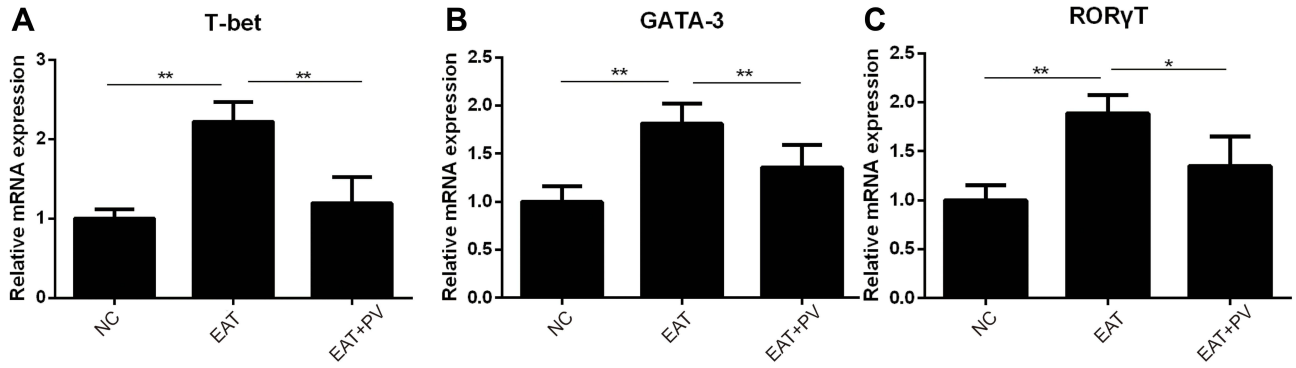

Figure 6 PV downregulated the mRNA expression of T-bet, GATA3 and RORγT in splenocytes of rats from different groups. The mRNA levels of T-bet (**A**), GATA3 (**B**) and RORγT (**C**) in splenocytes harvested from rats were determined using PCR (n=6 in each group). The data are presented as the mean ± SD and were derived from three independent experiments. Statistical comparisons among groups were performed using ANOVA. *P <0.05; **P< 0.01.

Abbreviations: NC, normal control group; EAT, experimental autoimmune thyroiditis rats administered PBS; EAT+PV, EAT rats administered PV extracts; T-bet, t-box expressed in T cells; GATA3, GATA binding protein 3; RORγT, retinoic acid receptor-related orphan nuclear receptor γt.

compared to the NC group. Consistent with the changes in the Th1, Th2 and Th17 cell subsets, PV administration significantly downregulated the mRNA expression of these transcription factors (P<0.01 for T-bet and GATA3, P<0.05 for RORγT).

To fully elucidate the mechanism of the PV-induced changes in the percentages of lymphocyte subsets, we inhibited HMGB1 in splenic mononuclear cells cultured in vitro by EP pretreatment and then determined the Th1, Th2 and Th17 cell proportions using flow cytometry. As expected, splenocytes from the in vitro-EAT group showed increased levels of HMGB1 (P<0.01) and TLR9 (P<0.01) mRNA expression compared with those from the in vitro-NC group (Figure 7A and B), accompanied by significant increases in the percentages of Th1, Th2, and Th17 cells compared with those in the in vitro-NC group (Figure 8A, B and C). In contrast, in non-inhibited cells (in vitro-EAT and in vitro-EAT+PV groups), PV pretreatment significantly reduced HMGB1 and TLR9 mRNA expression (Figure 7, P<0.01), accompanied by decreases in the percentages of Th1, Th2 and Th17 cells. In HMGB1^{-}inhibited cells treated with EP (in vitro-EAT+EP and in vitro-EAT+PV+EP groups), the mRNA expression of HMGB1 and TLR9 and the

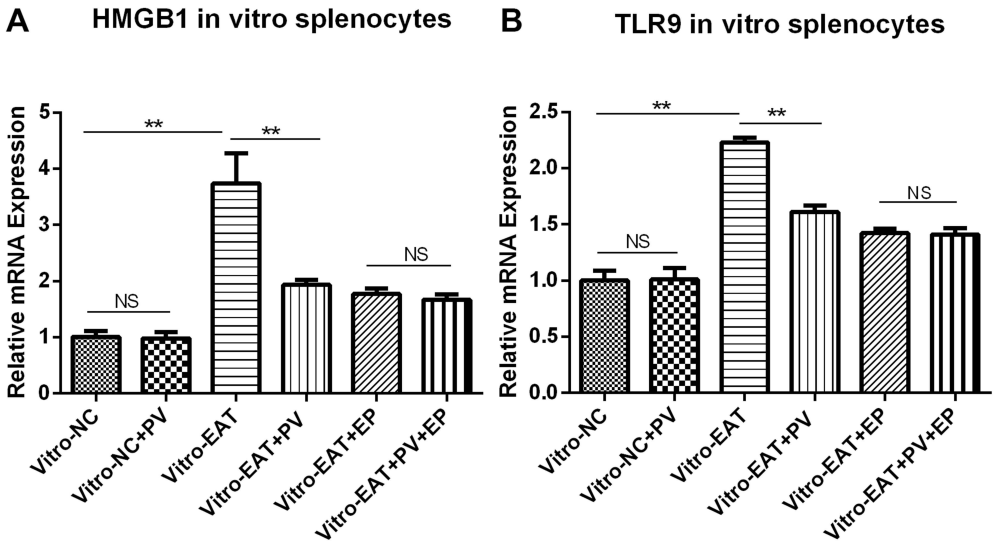

Figure 7 PV decreased the mRNA levels of HMGB1 and TLR9 in splenocytes cultured in vitro. The relative levels of HMGB1 (**A**) and TLR9 (**B**) mRNA in splenocytes cultured in vitro were determined using PCR. The data are presented as the mean ± SD and were derived from three independent experiments. Statistical comparisons among groups were performed using ANOVA. **P<0.01.

Abbreviations: NS, no significant difference. NC, spleen cells from rats in normal control group; NC+PV, spleen cells from rats in normal control group and treated with PV; EAT, spleen cells from rats in EAT group; EAT+PV, spleen cells from rats in EAT group and treated with PV; EAT+EP, spleen cells from rats in EAT group and treated with ethyl pyruvate; EAT+EP+PV, spleen cells from EAT group treated with ethyl pyruvate combined PV.

percentages of Th1 and Th17 cells were not significantly different, regardless of whether the cells were treated with PV (Figure 8, P>0.05). Notably, PV decreased the proportion of the Th2 cell subset in EP-pretreated cells, potentially because the differentiation of activated $CD4^+$ T cells depends upon the expression of specific transcription factors and cytokines and PV may stimulate Th2 cells by targeting other cytokines.

Discussion

In this study, Tg+NaI-immunized Lewis rats and LPS +NaI-induced TFCs were used as experimental models to explore the effects of PV on AIT and associated mechanisms in vivo and in vitro. The bioactive components of PV were identified using UPLC-ESI-MS before administration to rats and TFCs to ensure replicability, and the results showed that rosmarinic acid was the main component of aqueous PV extracts. PV exerted a therapeutic effect on AIT, and in vivo and in vitro, the PV-mediated inhibition of HMGB1 decreased the expression of proinflammatory cytokines, suppressed the downstream proteins in the HMGB1-TLR9 signaling pathway, and downregulated the proportions of Th1, Th2 and Th17 cells among splenocytes. Based on these findings, HMGB1 downregulation is the mechanism by which PV exerts its effects on AIT.

AIT development depends on an immune defect in an individual with a specific genetic background together with environmental factors. Iodine is a major environmental cause of AIT,[14] and Tg is an effective autoantigen stimulator.[15] An EAT model was established by excessive iodine intake and Tg injection in Lewis rats, which has been considered representative of human AIT for decades.[16] In this study, the therapeutic effects of PV on AIT were detected using Tg-induced Lewis rats. As expected, both the inflammatory cell infiltration and elevated serum antibody levels in EAT rats were remarkably alleviated by PV treatment. These results were consistent with previous clinical[17] and experimental[13] studies and confirmed the therapeutic effect of PV on EAT.

HMGB1 is a ubiquitous nuclear protein that functions as a DNA chaperone and participates in a number of activities in the nucleus under normal conditions. Under stress conditions, such as infection, ischemia, or injury, HMGB1 is also translocated into the extracellular space, where it functions as a DAMP that alerts nearby cells and the immune system to immediate danger, triggering inflammation.[18] Receptors for advanced glycation end products, TLR2, TLR4, and TLR9 have been identified as extracellular HMGB1 receptors. Among them, TLR9 mediates recognition of DNA viruses and CpG-containing oligodeoxynucleotides (CpG-ODNs) that induces type I interferon (IFN) production in plasmacytoid dendritic cells (pDCs), which is important for the pathogenesis of autoimmunity.[19] Therefore, the HMGB1/TLR9 pathway may play an important role in the pathogenesis of thyroiditis. LPS-induced TFCs were also used to model thyroiditis in vitro and to explore whether HMGB1 is involved in the therapeutic effect of PV on AIT. The mRNA and protein levels of HMGB1 in the thyroid and the level of secreted HMGB1 in the serum were significantly increased in the EAT group compared to the NC group in vivo; however, treatment with PV effectively reversed these changes. In addition, in vitro, LPS and NaI triggered increases in HMGB1 mRNA and protein expression in cells and HMGB1 secretion into the supernatant. Our results are similar to those of previous studies by Lee[20] and Wang,[21] which reported that LPS induces the extracellular release of HMGB1 in microglia and human intestinal epithelial cell lines (SW480 cells). As expected, in this study, treatment with PV effectively reduced the levels of HMGB1 in vitro. Therefore, HMGB1 participates in the pathogenesis of AIT, and PV has the potential to inhibit HMGB1 expression in AIT.

The current study also investigated whether the anti-inflammatory effect of PV was mediated by the inhibition of the TLR9/MyD88 signaling pathway. HMGB1 interacts with TLR9 to activate the NF-κB pathway and then produces cytokines and chemokines involved in inflammatory and immune responses.[22] Furthermore, previous studies[14] have shown that the persistent secretion of proinflammatory cytokines, such as TNF-α, IL-6, IL-1β and MCP-1, plays an essential role in AIT animal models. Consistent with the results reported by Teng and Xiao,[23,24] we observed increased expression of proinflammatory cytokines in Tg+NaI-induced Lewis rats and LPS+NaI-induced TFCs; higher concentrations of proinflammatory cytokines have been shown to regulate organ damage in AIT animal models,[14] and the overexpression of TNF-α, IL-6, IL-1β and MCP-1 in vivo and in vitro was reversed by PV. Our results indicate that PV administration inhibits the inflammatory response and cytokine production.

Excessively stimulated $CD4^+$ T cells are known to play the main role in the pathogenesis of AIT, and abnormally elevated percentages of Th1, Th2 and Th17 lymphocytes lead to autoimmune disorders in individuals with AIT.[3] Extracellular HMGB1 functions as a powerful mediator of

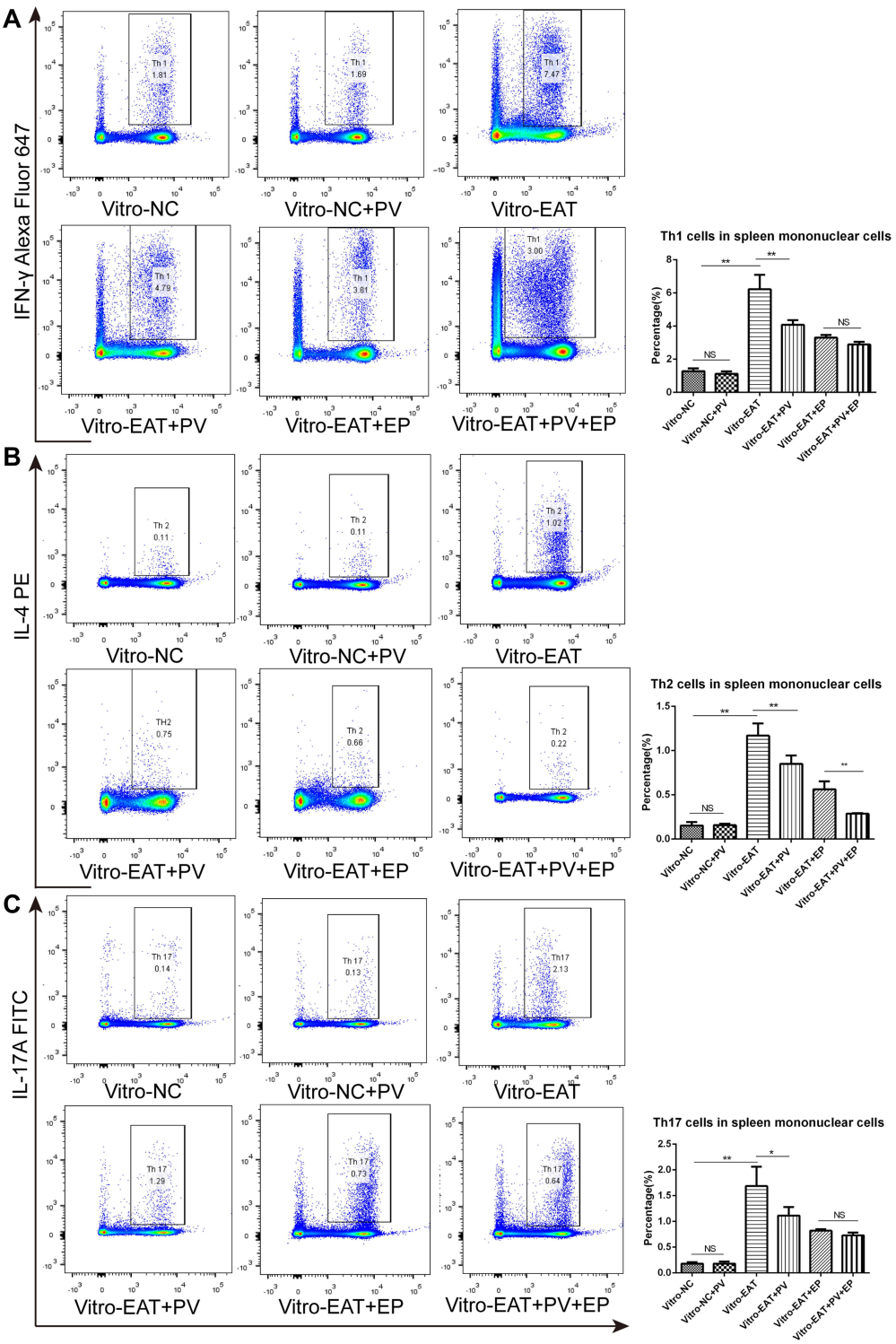

Figure 8 PV reduced the proportions of Th1/Th2/Th17 cells among splenocytes by inhibiting the HMGB1 pathway. Representative flow charts showing percentages of splenic Th1 (**A**), Th2 (**B**) and Th17 (**C**) cells with the corresponding column graphs. Subsets of Th1/Th2/Th17 cells in the $CD4^+$ gate were analyzed by performing intracellular staining for IFN-γ/ IL-4/ IL-17A in splenocytes cultured in vitro (left panels). The data are presented as the mean ± SD and were derived from three independent experiments. Pairwise statistical comparisons among groups were performed using ANOVA and Bonferroni corrections. *P<0.05; **P<0.01.

Abbreviations: NS, no significant difference. NC, spleen cells from rats in normal control group; NC+PV, spleen cells from rats in normal control group and treated with PV; EAT, spleen cells from rats in EAT group; EAT+PV, spleen cells from rats in EAT group and treated with PV; EAT+EP, spleen cells from rats in EAT group and treated with ethyl pyruvate; EAT+EP+PV, spleen cells from EAT group treated with ethyl pyruvate combined PV.

inflammation and is important in the proliferation, activation and suppression of naive $CD4^+$ T cells.[25] Therefore, the percentages of Th1, Th2 and Th17 cells in splenocytes from EAT rats were also measured in this study. The proportions of Th1 ($CD4^+$ IFN-γ^+), Th2 ($CD4^+$ IL-4^+) and Th17 ($CD4^+$ IL-17^+) cells were significantly increased in EAT rats, whereas the Th1, Th2 and Th17 proportions were significantly reduced after PV treatment.

We used an HMGB1 inhibitor, EP, to interfere with HMGB1 expression in vitro to determine whether HMGB1 is a druggable target of PV and whether the reductions in TLR9 and MyD88 expression, the decreases in proinflammatory cytokines and the alleviation of changes in the Th1, Th2 and Th17 subsets were mediated by HMGB1. As mentioned above, the findings indicated that PV decreased TLR9 and MyD88 expression in the thyroid, proinflammatory cytokine levels in the serum and Th1, Th2 and Th17 subset percentages through HMGB1. In summary, PV could play an important role in the treatment of thyroiditis by inhibiting the HMGB1/TLR9 pathway.

The present study had several limitations. First, the aqueous extract of PV was a mixture. We could not separate or quantify each compound with current technology. Therefore, we could not confirm that the attenuation of thyroiditis and inhibition of HMGB1/TLR9 signaling by PV were mediated by rosmarinic acid or any other specific component. Second, our results from the in vitro experiments were obtained with only a TFC line and should be confirmed with other thyroid follicular epithelial cells. In addition, EAT rats were not treated with an HMGB1 inhibitor in vivo because EP is generally administered by injection according to the published literature,[26,27] while PV was administered by oral gavage in this study and is similarly administered in clinical practice. Therefore, we administered EP only in vitro to avoid experimental error caused by different administration methods.

Conclusions

In conclusion, we focused on the therapeutic effect and molecular mechanism of PV in AIT using an EAT rat model and LPS+NaI-induced TFCs. Our study is the first to show that decreased expression of HMGB1/TLR9/MyD88 pathway components may be involved in PV-induced thyroiditis attenuation and downregulation of proinflammatory cytokines and Th1, Th2 and Th17 cell subsets in EAT. This study provides insights into the immunopathogenesis of AIT and suggests the potential therapeutic value of PV in AIT, with HMGB1 identified as a potential target.

Ethical Approval and Informed Consent

All experimental procedures were approved by the Experimental Animal Management Committee of Shandong Provincial Hospital according to the Guideline for Ethical Review of Animal Welfare (GB/T 35892–2018).

Acknowledgments

This work was supported by Prof. Xia Zhong at Shandong Provincial Hospital, affiliated to Shandong First Medical University, and Guiyang Xintian Pharmaceutical Co., Ltd. (Guizhou, China). We thank all technicians at the Experimental Animal Center of Shandong Provincial Hospital for their assistance. We would also like to thank Dr.Xin Shen for her advice and help in designing figure layout and writing manuscript.

Disclosure

The extracts of PV were prepared by Guiyang Xintian Pharmaceutical Co., Ltd. However, apart from that, no other relationships that might lead to a conflict of interest or artificial bias of the results exist.

References

1. Burek CL, Talor MV. Environmental triggers of autoimmune thyroiditis. *J Autoimmun*. 2009;33(3–4):183–189. doi:10.1016/j.jaut.2009.09.001
2. Dong YH, Fu DG. Autoimmune thyroid disease: mechanism, genetics and current knowledge. *Eur Rev Med Pharmacol Sci*. 2014;18(23):3611–3618. doi:10.2147/DDDT.S320320
3. Pyzik A, Grywalska E, Matyjaszek-Matuszek B, et al. Immune disorders in Hashimoto's thyroiditis: what do we know so far? *J Immunol Res*. 2015;2015:979167. doi:10.1155/2015/979167
4. Ralli M, Angeletti D, Fiore M, et al. Hashimoto's thyroiditis: an update on pathogenic mechanisms, diagnostic protocols, therapeutic strategies, and potential malignant transformation. *Autoimmun Rev*. 2020;19(10):102649. doi:10.1016/j.autrev.2020.102649
5. Yang H, Wang H, Czura CJ, et al. HMGB1 as a cytokine and therapeutic target. *J Endotoxin Res*. 2002;8(6):469–472. doi:10.1179/096805102125001091
6. Li C, Peng S, Liu X, et al. Glycyrrhizin, a Direct HMGB1 Antagonist, Ameliorates Inflammatory Infiltration in a Model of Autoimmune Thyroiditis via Inhibition of TLR2-HMGB1 Signaling. *Thyroid*. 2017;27(5):722–731. doi:10.1089/thy.2016.0432
7. Harris HE, Andersson U, Pisetsky DS. HMGB1: a multifunctional alarmin driving autoimmune and inflammatory disease. *Nat Rev Rheumatol*. 2012;8(4):195–202. doi:10.1038/nrrheum.2011.222
8. Beutler B. Inferences, questions and possibilities in Toll-like receptor signalling. *Nature*. 2004;430(6996):257–263. doi:10.1038/nature02761
9. Peng S, Li C, Wang X, et al. Increased Toll-Like Receptors Activity and TLR Ligands in Patients with Autoimmune Thyroid Diseases. *Front Immunol*. 2016;7:578. doi:10.3389/fimmu.2016.00578

10. Fazal H, Abbasi BH, Ahmad N, et al. Exogenous melatonin trigger biomass accumulation and production of stress enzymes during callogenesis in medicinally important Prunella vulgaris L. (Selfheal). *Physiol Mol Biol Plants*. 2018;24(6):1307–1315. doi:10.1007/s12298-018-0567-7
11. Du J, Leilei B, Yanrong X. Effect of Xiakucao Granules Combined with Danzhi Xiaoyao Powder Granules Combined with western medicine on Hashimoto's thyroiditis and hypothyroidism. *Beijing Traditional Chine Med*. 2020;07(39):738–741.
12. Ming WE, Gu QR, Li HL. Clinical study on adjuvant treatment of Hashimoto's thyroiditis with Xiakucao capsule. *New Traditional Chinese Medicine*. 2020;19(52):91–94. doi:10.13457/j.cnki.jncm.2020.19.02
13. Qiu H, Zhang J, Guo Q, et al. Prunella vulgaris L. attenuates experimental autoimmune thyroiditis by inducing indoleamine 2,3-dioxygenase 1 expression and regulatory T cell expansion. *Biomed Pharmacother*. 2020;128:110288. doi:10.1016/j.biopha.2020.110288
14. Sun X, Guan H, Peng S, et al. Growth arrest-specific protein 6 (Gas6) attenuates inflammatory injury and apoptosis in iodine-induced NOD.H-2(h4) mice. *Int Immunopharmacol*. 2019;73:333–342. doi:10.1016/j.intimp.2019.04.038
15. Wei S, Guanghua S, Bin H. Experimental autoimmune thyroiditis induced by iodine and thyroglob zulin in rats. *Chine J Int Med*. 2000;12(2000):48–49. doi:10.3760/j.issn:0578-1426.2000.12.020
16. Cui SL, Yu J, Shoujun L. Iodine Intake Increases IP-10 Expression in the Serum and Thyroids of Rats with Experimental Autoimmune Thyroiditis. *Int J Endocrinol*. 2014;2014:581069. doi:10.1155/2014/581069
17. Jianmin R, Maohong W. Clinical observation of Xiakucao oral liquid in adjuvant treatment of Hashimoto's disease with hypothyroidism. *J China Japan Friendship Hospital*. 2006;5(20):315. doi:10.3969/j.issn.1001-0025.2006.05.020
18. Venereau E, De Leo F, Mezzapelle R, et al. HMGB1 as biomarker and drug target. *Pharmacol Res*. 2016;111:534–544. doi:10.1016/j.phrs.2016.06.031
19. Kumagai Y, Takeuchi O, Akira S. TLR9 as a key receptor for the recognition of DNA. *Adv Drug Deliv Re*. 2008;60(7):795–804. doi:10.1016/j.addr.2007.12.004
20. Lee S, Nam Y, Koo JY, et al. A small molecule binding HMGB1 and HMGB2 inhibits microglia-mediated neuroinflammation. *Nat Chem Biol*. 2014;10(12):1055–1060. doi:10.1038/nchembio.1669
21. Wang FC, Pei JX, Zhu J, et al. Overexpression of HMGB1 A-box reduced lipopolysaccharide-induced intestinal inflammation via HMGB1/TLR4 signaling in vitro. *World J Gastroenterol*. 2015;21:7764–7776. doi:10.3748/wjg.v21.i25.7764
22. Kang R, Chen R, Zhang Q, et al. HMGB1 in health and disease. *Mol Aspects Med*. 2014;40:1–116. doi:10.1016/j.mam.2014.05.001
23. Peng S, Li C, Wang X, et al. Increased Toll-Like Receptors Activity and TLR Ligands in Patients with Autoimmune Thyroid Diseases. *Front Immunol*. 2016;7:578. doi:10.3389/fimmu.2016.00578
24. Liu J, Mao C, Dong L, et al. Excessive Iodine Promotes Pyroptosis of Thyroid Follicular Epithelial Cells in Hashimoto's Thyroiditis Through the ROS-NF-kappaB-NLRP3 Pathway. *Front Endocrinol*. 2019;10:778. doi:10.3389/fendo.2019.00778
25. Dumitriu IE, Baruah P, Valentinis B, et al. Release of high mobility group box 1 by dendritic cells controls T cell activation via the receptor for advanced glycation end products. *J Immunol*. 2005;174(12):7506–7515. doi:10.4049/jimmunol.174.12.7506
26. Dave SH, Tilstra JS, Matsuoka K, et al. Ethyl pyruvate decreases HMGB1 release and ameliorates murine colitis. *J Leukoc Biol*. 2009;86(3):633–643. doi:10.1189/jlb.1008662
27. Su X, Wang H, Zhao J, et al. Beneficial effects of ethyl pyruvate through inhibiting high-mobility group box 1 expression and TLR4/NF-kappaB pathway after traumatic brain injury in the rat. *Mediators Inflamm*. 2011;2011:807142. doi:10.1155/2011/807142